Electron beam–plasma interaction and ion-acoustic solitary waves in plasmas with a superthermal electron component

2010 Plasma Phys. Control. Fusion 52 075009

(http://iopscience.iop.org/0741-3335/52/7/075009)

IOP PUBLISHING PLASMA PHYSICS AND CONTROLLED FUSION

Plasma Phys. Control. Fusion **52** (2010) 075009 (19pp) doi:10.1088/0741-3335/52/7/075009

Electron beam–plasma interaction and ion-acoustic solitary waves in plasmas with a superthermal electron component

N S Saini and I Kourakis

Centre for Plasma Physics, Department of Physics and Astronomy, Queen's University Belfast, BT7 1NN, Northern Ireland, UK

E-mail: nssaini@yahoo.com, ns.saini@qub.ac.uk and i.kourakis@qub.ac.uk

Received 2 December 2009, in final form 6 May 2010
Published 17 June 2010
Online at stacks.iop.org/PPCF/52/075009

Abstract

The study of non-Maxwellian plasmas is crucial to the understanding of space and astrophysical plasma dynamics. In this paper, we investigate the existence of arbitrary amplitude ion-acoustic solitary waves in an unmagnetized plasma consisting of ions and excess superthermal electrons (modelled by a kappa-type distribution), which is penetrated by an electron beam. A kappa (κ-) type distribution is assumed for the background electrons. A (Sagdeev-type) pseudopotential formalism is employed to derive an energy-balance like equation. The range of allowed values of the soliton speed (Mach number), wherein solitary waves may exist, is determined. The Mach number range (allowed soliton speed values) becomes narrower under the combined effect of the electron beam and of the superthermal electrons, and may even be reduced to nil (predicting no solitary wave existence) for high enough beam density and low enough κ (significant superthermality). For fixed values of all other parameters (Mach number, electron beam-to-ion density ratio and electron beam velocity), both soliton amplitude and (electric potential perturbation) profile steepness increase as κ decreases. The combined occurrence of small-amplitude negative potential structures and larger amplitude positive ones is pointed out, while the dependence of either type on the plasma parameters is investigated.

1. Introduction

The existence of nonlinear ion-acoustic (IA) solitary structures in different plasma environments has been confirmed theoretically as well as experimentally by a number of researchers [1–3]. It is established that stationary nonlinear localized electrostatic (ES) waves may be excited when an electron beam is injected into a plasma [4]. The presence of electron beams is also clearly indicated by space observations in the upper layer of the magnetosphere,

where a coexistence of two different electron populations (say, warm energetic ones and cold, i.e. inertial electrons) is reported by various satellite missions (the S3-3 [5], Viking [6], the FAST at the auroral region [7, 8], GEOTAIL [8] and POLAR [9]). Interestingly, the GEOTAIL mission has observed the existence of solitary waves propagating at a speed much slower than the thermal speed of the electrons [10, 11]. These plasma conditions have also been produced in the laboratory [12–15].

Focusing on nonlinear ES excitations, it is well known that the injection of an electron beam into a plasma strongly affects the conditions for the occurrence of solitary waves and may modify their properties. This is shown either by small-amplitude solitary wave theory (based on a reductive perturbation method) [16–18] or by more rigorous studies of large amplitude excitations (described by a pseudopotential approach) [19–21]. Such theoretical considerations have later been extended to numerical simulations [22] of electron-acoustic waves (related to broadband electrostatic noise, BEN, in the Earth's auroral region) [23]. The effect(s) of the electron beam density, ion temperature and/or electron beam temperature has (have) been investigated on the characteristics of small and large amplitudes ES solitary waves on either IA [20] or electron-acoustic scales in electron beam–plasma systems [24–26]. A recent combined study of nonlinear ion- and electron-acoustic solitary waves in multi-component space plasmas in the presence of ion and electron beams has shown that three types of solitary waves may exist; namely, slow IA, IA and electron-acoustic solitons were found above a critical value of the Mach number [26]. Considering higher order nonlinearity effects in a plasma consisting of adiabatic warm ions, nonisothermal electrons and weakly relativistic electron beam, it is observed that the amplitude and shape of IA solitary wave may be significantly modified [27]. The vast majority of existing investigations of ES excitations (e.g., cited above) have considered a Maxwellian distribution of the background electron species. Going beyond this traditional textbook description is part of our scope here, well motivated by Space observations, as we shall discuss below.

The presence of superthermal particles in space plasma environments [28–34] and laboratory experiments [35–39] has been reported by a number of observations. The combined effect of wave–particle interaction and external forces on natural space environment plasmas is one main cause for the generation of superthermal particles. Due to the presence of superthermal electrons, a high-energy tail appears in the distribution function, which is conveniently modelled via a non-Maxwellian (generalized kappa) distribution. In a variety of space plasma environments, the kappa-type distribution has been suggested as more appropriate for real data analysis [40–44] (in comparison, that is, with the usual Maxwellian background assumption).

The three dimensional kappa distribution function is given by [42, 45]

$$f_\kappa(v) = \frac{n_0}{(\pi\kappa\theta^2)^{3/2}} \frac{\Gamma(\kappa+1)}{\Gamma(\kappa-\frac{1}{2})} \left(1+\frac{v^2}{\kappa\theta^2}\right)^{-(\kappa+1)}, \tag{1}$$

where v and n_0 are the velocity and equilibrium number density of the species, respectively. $\theta = [(1-(3/2\kappa))(2k_B T/m)]^{1/2}$ is the effective thermal speed, modified by the spectral index $\kappa(>3/2)$, where T is the kinetic temperature and m is the mass of the species. Using the kappa distribution function and integrating over velocity space, one can obtain the number density of the corresponding plasma species. For very large values of κ, the velocity distribution function approaches a Maxwellian distribution.

We shall here rely on the original expression (1) for the κ distribution [40]. It may be added, for the sake of rigour and completeness, that a number of alternative forms have appeared in the past, bearing similar qualitative features (yet slightly different algebraic structure); we refer the reader to the critical discussion in the recent references [45, 46]. Another candidate for

the modelling of nonthermal plasmas, the Tsallis ('q-Gaussian') distribution [47], has been shown to lie in the foundation of non-extensive thermodynamics and is now gaining ground in modelling non-Maxwellian dynamics of many-body systems (plasmas and others) [47, 48]. It can be claimed, from first principles, that the kappa distribution is qualitatively analogous to the Tsallis distribution. Despite a number of works that have addressed the apparent ubiquity of the kappa distribution(s) in various plasma contexts [49–51], there is at this stage no comprehensive theory relating this family of distributions to the fundamental underlying physics. Quite remarkably, a recent study just brought to our attention [46] claims to establish a rigorous link between the κ (family of) distribution(s) and the Tsallis distribution. This analogy is, however, certainly not algebraically straightforward, and still appears to be a controversial topic.

In account of the ubiquitous existence of superthermal electrons (in space [28–34, 49–51] and in laboratory [35–39] plasmas) and in relation with the associated observation of solitary structures [52–54], we have undertaken in the text to follow a study of the effect of superthermality on IA solitary waves in the presence of an electron beam in superthermal plasmas. We shall derive an energy-balance-like equation for solitary waves and will investigate the parametric regime for their existence, in relation to different types of excitations. The effect of the electron beam characteristics, as well as of the superthermality of the background, will be discussed.

The layout of this paper is organized as follows. The model equations are presented in section 2. In section 3, we reduce the arbitrary amplitude solitary wave problem to a mechanical-energy-balance-analogue equation by adopting the established pseudopotential (Sagdeev) approach. In section 4, we shall investigate the conditions for the existence of solitary structures. The effect of superthermality and of the beam parameters (electron beam-to-ion density ratio and electron beam velocity) on the characteristics of solitary waves will be discussed in section 5. Finally, the concluding section 6 will summarize the results presented in this paper.

2. Two-fluid beam–plasma model

We consider a collisionless and unmagnetized plasma consisting of three components, namely cold ions (charge $q_\mathrm{i} = Ze$, mass m_i), electron beam (charge $q_\mathrm{e} = -e$, mass m_e) and superthermal electrons. The former two species (ions and electron beam) are described by a set of fluid moment equations, while the latter (electrons) are modelled by a kappa velocity distribution. We shall adopt a one-dimensional description for simplicity.

The fluid equations read, for the ions,

$$\frac{\partial n_\mathrm{i}}{\partial t} + \frac{\partial (n_\mathrm{i} u_\mathrm{i})}{\partial x} = 0, \tag{2}$$

$$\frac{\partial u_\mathrm{i}}{\partial t} + u_\mathrm{i}\frac{\partial u_\mathrm{i}}{\partial x} = -\frac{q_\mathrm{i}}{m_\mathrm{i}}\frac{\partial \Phi}{\partial x}, \tag{3}$$

and for the electron beam,

$$\frac{\partial n_\mathrm{b}}{\partial t} + \frac{\partial (n_\mathrm{b} u_\mathrm{b})}{\partial x} = 0, \tag{4}$$

$$\frac{\partial u_\mathrm{b}}{\partial t} + u_\mathrm{b}\frac{\partial u_\mathrm{b}}{\partial x} = \frac{e}{m_\mathrm{e}}\frac{\partial \Phi}{\partial x}. \tag{5}$$

The four equations are coupled through the Poisson equation,

$$\frac{\partial^2 \Phi}{\partial x^2} = -4\pi e(n_\mathrm{i} Z - n_\mathrm{e} - n_\mathrm{b}), \tag{6}$$

where n_α (α = i, e, b), u_i, u_b and Φ denote the number density of each species, the ion mean velocity, the beam velocity and the ES potential, respectively. The assumption of charge neutrality at equilibrium, $n_{\mathrm{i}0}Z = n_{\mathrm{e}0} + n_{\mathrm{b}0}$, implies

$$Z = \alpha + \nu, \tag{7}$$

where we have defined the parameters

$$\alpha = n_{\mathrm{e}0}/n_{\mathrm{i}0} \qquad \text{and} \qquad \nu = n_{\mathrm{b}0}/n_{\mathrm{i}0}. \tag{8}$$

The electron number density is

$$n_\mathrm{e} = n_{\mathrm{e}0}\left[1 - \frac{e\Phi}{(\kappa - \frac{3}{2})k_\mathrm{B}T_\mathrm{e}}\right]^{-\kappa+1/2}, \tag{9}$$

where the real parameter κ measures the deviation from Maxwellian equilibrium (recall that $\kappa > 3/2$ in order for a physically meaningful thermal speed to be defined). We stress the fact that no charge-neutrality condition is imposed on the plasma state off-equilibrium, thus allowing the number densities of all species to evolve dynamically in response to potential variations, as dictated by Poisson's law.

The electron beam velocity $u_{\mathrm{b}0}$ will be later incorporated in the description via the boundary conditions (see in the next section). We shall assume a finite-yet-negligible overall charge current $j = n_{\mathrm{b}0}u_{\mathrm{b}0} \simeq 0$, in order for the ES character of the excitations to be preserved, i.e. for the right-hand side (rhs) of Ampère's law to vanish [55]. Thus, we shall restrict our beam density and velocity parameters to very low values, i.e. by taking $\nu U_0 \ll 1$, where $U_0 = u_{\mathrm{b}0}/c_\mathrm{s}$ is the reduced beam velocity.

Normalizing by appropriate scaling quantities (to be determined below), we may cast the system of two-fluid-Poisson equations in a dimensionless form. The reduced equations are presented in the following. For the ions:

$$\frac{\partial n}{\partial t} + \frac{\partial (nu)}{\partial x} = 0, \tag{10}$$

$$\frac{\partial u}{\partial t} + u\frac{\partial u}{\partial x} = -\frac{\partial \phi}{\partial x}; \tag{11}$$

for the electron beam:

$$\frac{\partial n_\mathrm{b}}{\partial t} + \frac{\partial (n_\mathrm{b}u_\mathrm{b})}{\partial x} = 0, \tag{12}$$

$$\frac{\partial u_\mathrm{b}}{\partial t} + u_\mathrm{b}\frac{\partial u_\mathrm{b}}{\partial x} = \frac{1}{\mu Z}\frac{\partial \phi}{\partial x}; \tag{13}$$

Poisson's equation becomes

$$\frac{\partial^2 \phi}{\partial x^2} = -n + \frac{\alpha}{Z}\left(1 - \frac{\phi}{\kappa - 3/2}\right)^{-\kappa+1/2} + \frac{n_\mathrm{b}}{Z}. \tag{14}$$

Here the fluid velocity u_i, the number density n_i and the ES potential Φ variables are scaled as $u = u_\mathrm{i}/c_\mathrm{s}$, $n = n_\mathrm{i}/n_{\mathrm{i}0}$ and $\phi = \Phi/\Phi_0$; we have defined the unperturbed ion density $n_{\mathrm{i}0}$. The beam variables are $\tilde{n_\mathrm{b}} = n_\mathrm{b}/n_{\mathrm{i}0}$ and $\tilde{u_\mathrm{b}} = u_\mathrm{b}/c_\mathrm{s}$; the tildes are dropped in equations (12)–(14) and henceforth. Space and time variables are scaled by the Debye length $\lambda_{\mathrm{D,e}} = (k_\mathrm{B}T_\mathrm{e}/4\pi Zn_{\mathrm{i}0}e^2)^{1/2}$, and the inverse ion plasma frequency $\omega_{\mathrm{p,i}}^{-1} = (4\pi n_{\mathrm{i}0}Z^2e^2/m_\mathrm{i})^{-1/2}$, respectively. Finally, $\mu = m_\mathrm{e}/m_\mathrm{i}$ ($\simeq 1/1836$), and the potential scale reads $\Phi_0 = k_\mathrm{B}T_\mathrm{e}/e$. The characteristic velocity scale (IA 'sound speed') used is $c_\mathrm{s} \equiv (Zk_\mathrm{B}T_\mathrm{e}/m_\mathrm{i})^{1/2}$.

We should point out, for rigour, that the latter (textbook) expression for the 'sound speed' c_s rigorously applies to an electron–ion plasma in which the electrons obey a Boltzmann

distribution. On the other hand, in nonthermal plasmas, Debye shielding is altered in a plasma with a κ distribution, and thus an effective κ-dependent Debye length is found [57]. Thus, the *true* sound speed in the plasma model under consideration, with an electron density as given by equation (9), is essentially κ-dependent and differs from c_s, as will be discussed below. The term 'real sound speed' will therefore be used below, where appropriate, to distinguish the true modified (κ-dependent) sound speed in our plasma system.

3. Pseudopotential approach

To obtain a solitary wave solution, we assume that all fluid variables in the evolution equations depend on a single variable $\xi = x - Mt$ (where M is the Mach number, i.e. the pulse propagation velocity normalized by the sound speed). This is the well-known pseudopotential method, leading to a number of ordinary differential equations (ODEs) in a variable of ξ. Now equations (10) to (14) take the form

$$-M\frac{\partial n}{\partial \xi} + \frac{\partial (nu)}{\partial \xi} = 0, \tag{15}$$

$$-M\frac{\partial u}{\partial \xi} + u\frac{\partial u}{\partial \xi} + \frac{\partial \phi}{\partial \xi} = 0, \tag{16}$$

$$-M\frac{\partial n_b}{\partial \xi} + \frac{\partial (n_b u_b)}{\partial \xi} = 0, \tag{17}$$

$$-M\frac{\partial u_b}{\partial \xi} + u_b\frac{\partial u_b}{\partial \xi} - \frac{1}{Z\mu}\frac{\partial \phi}{\partial \xi} = 0, \tag{18}$$

$$\frac{\partial^2 \phi}{\partial \xi^2} = -n + \frac{Z-\nu}{Z}\left(1 - \frac{\phi}{\kappa - 3/2}\right)^{-\kappa+1/2} + \frac{n_b}{Z}. \tag{19}$$

Note that the rhs of the latter (pseudo-) equation of motion for the moving electric potential disturbance vanishes at equilibrium ($n \to 1$, $u \to 0$, $n_b \to \nu$ and $\phi \to 0$).

After integrating equations (15) to (18) and applying appropriate boundary conditions for localized perturbations, namely, $n \to 1$, $u \to 0$, $n_b \to \nu$, $u_b \to U_0$ and $\phi \to 0$ at $\xi \to \pm\infty$, we obtain

$$u = M\left(1 - \frac{1}{n}\right), \tag{20}$$

and

$$-Mu + \frac{u^2}{2} = -\phi. \tag{21}$$

From equations (20) and (21), we find

$$n = \frac{1}{\sqrt{1 - \frac{2\phi}{M^2}}}. \tag{22}$$

The reality condition $M^2 \geqslant 2\phi$ is to be imposed here; note that this requirement of a physically realistic density limits positive potential values only. From equations for the electron beam, we find

$$n_b = \nu\frac{M - U_0}{M - u_b}, \tag{23}$$

and

$$\frac{1}{2}u_b^2 - Mu_b + MU_0 - \frac{U_0^2}{2} - \frac{1}{Z\mu}\phi = 0. \tag{24}$$

From equations (23) and (24), the density of electron beam is given as

$$n_b = \frac{\nu}{\sqrt{1 + \frac{2\phi}{Z\mu(M-U_0)^2}}}. \tag{25}$$

We emphasize the fact that equations (22) and (25) act as energy criteria, impose boundaries to our region of potential ϕ values of importance in the following. In specific (due to reality requirements) positive solutions (for ϕ) are limited by

$$\phi \leqslant \frac{M^2}{2}, \tag{26}$$

while negative solutions for ϕ are limited by

$$|\,\phi\,| \leqslant \frac{Z\mu(M-U_0)^2}{2} \approx \frac{Z\mu M^2}{2} \qquad (\text{for } U_0 \ll M). \tag{27}$$

Given the smallness of μ, one expects small values of the negative potential pulses (see the figures).

Substituting equations (22) and (25) into equation (19), multiplying the resulting equation by $\mathrm{d}\phi/\mathrm{d}\xi$, integrating and applying the boundary conditions, $\mathrm{d}\phi/\mathrm{d}\xi \to 0$ at $\xi \to \pm\infty$, we get

$$\frac{1}{2}\left(\frac{\mathrm{d}\phi}{\mathrm{d}\xi}\right)^2 + V(\phi, M) = 0, \tag{28}$$

where the pseudopotential $V(\phi, M)$ is given by

$$V(\phi, M) = M^2\left(1 - \sqrt{1 - \frac{2\phi}{M^2}}\right) + \frac{Z-\nu}{Z}\left[1 - \left(1 - \frac{\phi}{\kappa - 3/2}\right)^{-\kappa+3/2}\right] + \nu\mu(M-U_0)^2\left[1 - \left(1 + \frac{2\phi}{Z\mu(M-U_0)^2}\right)^{1/2}\right]. \tag{29}$$

Equation (28) can be regarded as the 'energy-balance equation' for an oscillating particle of unit mass, with position ϕ, time ξ, velocity $\mathrm{d}\phi/\mathrm{d}\xi$ and potential $V(\phi, M)$ given by equation (29). We recall, in view of the forthcoming analysis, that the Maxwellian limit [2] is clearly recovered for $\kappa \to \infty$ and $\nu \to 0$.

4. ES solitary waves: conditions for occurrence

For solitary wave solutions of equation (28) to exist, the following requirements must be satisfied:

(i) $V(\phi = 0, M) = \mathrm{d}V(\phi, M)/\mathrm{d}\phi\big|_{\phi=0} = 0$ (at the origin), which indicates that both the electric field and the charge density be zero far from the localized positive/negative potential solitary structures,

(ii) $\mathrm{d}^2V(\phi, M)/\mathrm{d}\phi^2\big|_{\phi=0} < 0$, so that the fixed point is unstable at the origin (i.e. $V(\phi, M)$ has a maximum at the origin) and

(iii) $V(\phi, M) < 0$ for $0 < |\phi| < |\phi_0|$; here ϕ_0 denotes the positive root ($\phi_{\max}$), for positive potential solitary waves (or conversely the negative root ($\phi_{\min}$), for negative potential solitary waves).

4.1. Mach number threshold M_1: the soliton existence condition

At equilibrium, equation (29) shows that $V(\phi = 0, M) = 0$ and $\mathrm{d}V(\phi = 0, M)/\mathrm{d}\phi = 0$. The condition for the existence of solitons can be found from the roots of $\mathrm{d}^2V(\phi, M)/\mathrm{d}\phi^2\big|_{\phi=0} = 0$ in terms of the Mach number M. The lower limit of the Mach number, say, $M = M_1$ is given by solving

$$\frac{1}{M^2} - \frac{Z-\nu}{Z}\frac{2\kappa-1}{2\kappa-3} + \frac{\nu}{\mu Z^2(M-U_0)^2} \leqslant 0, \tag{30}$$

where the equality holds for, say, $M = M_1$.

It may be appropriate to discuss the ordering of different terms here.

Maxwellian e–i plasma limit. First, setting $\nu \to 0$ and $\kappa \to \infty$ in equation (30), we readily recover the limit $M_1 = 1$, establishing the known supersonic character of IA solitary waves in ordinary e–i plasmas [2].

Kappa (superthermality) effect (no beam). Now, 'switching on' superthermality ($\kappa < \infty$), but still keeping the beam absent ($\nu = 0$), we see that an immediate consequence of the kappa-distributed background is to lower the sound speed to, say, $M_1^{(\kappa)} = \sqrt{(2\kappa-3)/(2\kappa-1)}$. Note that $M_1^{(\kappa)} < 1$. In fact, the sound speed remains in the vicinity of 1 for large κ, yet reduces down to very low values below, say, $\kappa = 6$ (and even vanishes for $\kappa \to 3/2$), as extensively discussed in Saini *et al* [44].

Beam effect (no kappa). Inversely, keeping for a minute the beam present ($\nu \neq 0$) but electrons Maxwellian ($\kappa = \infty$), the 'sonic' threshold changes to, say, $M_1^{(\nu)} \simeq \sqrt{1+\nu/\mu Z^2}$ (recalling that $U_0 \ll 1 < M$). Note that $M_1^{(\nu)} > 1$. At this stage, one might be tempted to argue that $\mu \simeq 1/1836 \ll 1$. However, we note that the ratio μ/ν is, in fact, much larger than unity, given the low values of ν ($\sim 10^{-4}$–10^{-5}) here considered for purely ES excitations (see discussion above). Thus, the effect of the beam is to increase the threshold for ES solitary waves to exist. In fact, it increases the value of the root of $V''(\phi)|_{\phi=0}$ on the M-axis (refer to the discussion in [56] and note figure 1 therein).

Combined beam-kappa effect. Concluding, we see that the combined effect of the electron beam *and* the superthermality of the background consists of a competition among the second and third term(s) in equation (30), which tends to allow for slower and faster, respectively, excitations to occur. To trace this effect qualitatively, we obtain the approximate root of equation (30):

$$M_1 \simeq \left(\frac{2\kappa-3}{2\kappa-1}\right)^{1/2}\left(1+\frac{\nu}{\mu Z^2}\right)^{1/2}, \tag{31}$$

i.e. $M_1 \simeq M_1^{(\kappa)} M_1^{(\nu)}$ (we have used $U_0 \ll M$ and $\nu \ll 1 \leqslant Z$).

A more rigorous approach consists of solving equation (30) numerically. The quartic polynomial equation (30) yields four roots; however, all the roots will not be physically acceptable, since only real positive roots are to be considered. A numerical investigation suggests that only one positive real root of M_1 exists for realistic finite values of the physical parameters. For instance, for $Z = 1$, $\nu = 0.000\,25$, $U_0 = 0.05$ and $\kappa = 3.5$, we find $M_1 = 1.002\,93$, which is greater than the IA speed in the Maxwellian case. In the absence of the electron beam (setting $\nu = 0$), equation (30) yields $M_1 = 0.816\,497$ which agrees with the value of the lower limit of the Mach number [44].

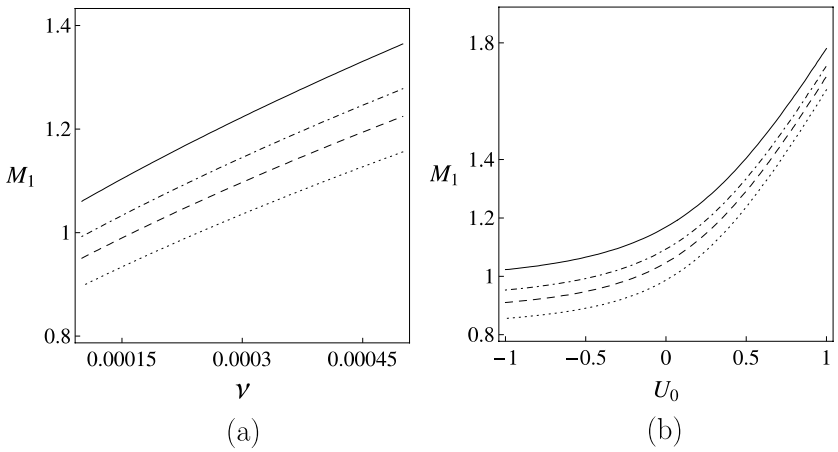

Figure 1. Variation of the Mach Number M_1 (lower velocity limit) (a) with ratio of density of electron beam to ion (ν) for $U_0 = 0.05$ and (b) with electron beam velocity (U_0) for $\nu = 0.000\,25$. From bottom to top, the dotted curve corresponds to $\kappa = 3.5$, dashed to $\kappa = 4.5$, dotted–dashed to $\kappa = 6$ and solid curve to $\kappa = 16$.

We have analysed numerically the variation of the lower velocity limit M_1 with density ratio of electron beam to ion (ν) for fixed values of κ, beam velocity U_0 and μ. From figure 1(a), it is seen that M_1 increases with increase in ν as well as the value of κ. A small value of κ represents more superthermal particles and thus an increase in superthermality lowers the value of M_1, as discussed above. In any case, the presence of the electron beam results in the sonic threshold M_1 exceeding the beam-free value (for e–i plasma), either with superthermal or with Maxwellian electrons.

Figure 1(b) shows the variation of the lower velocity limit M_1 with electron beam velocity U_0 for fixed values of κ, ν and μ. We see that the critical Mach number M_1 increases with an increase in beam velocity (for positive U_0) and/or with an increase in the value of κ. We may stress that both positive and negative values of the beam velocity U_0 were considered in this figure, the former (latter) corresponding to ES solitary wave propagation parallel to (opposite to) the beam direction of flow. In the negative region, i.e. for counter-propagating ES solitary waves, we see that the effect is reversed, that is, an increase in the (absolute) value of U_0 leads to a decrease in M_1, hence to a wider—more extended—region of permitted speed M values.

4.2. Upper Mach number limit M_2: the infinite compression limit

For solitary waves to exist, an upper velocity limit arises from the physical requirement of a real ion number density, as given by equation (22). The upper velocity limit (say M_2) can be found by imposing the requirement $V(\phi = M^2/2) \geqslant 0$ and is therefore obtained numerically from the following equation,

$$M_2^2 + \frac{Z-\nu}{Z}\left[1 - \left(1 - \frac{M_2^2}{2\kappa - 3}\right)^{-\kappa+3/2}\right] + \nu\mu(M_2 - U_0)^2\left[1 - \left(1 + \frac{M_2^2}{Z\mu(M_2 - U_0)^2}\right)^{1/2}\right] = 0. \tag{32}$$

Let us consider various effects in equation (32), by isolating the different terms therein. First, by taking both $\nu = 0$ (no beam) and $\kappa \to \infty$ (Maxwellian electrons), we recover the

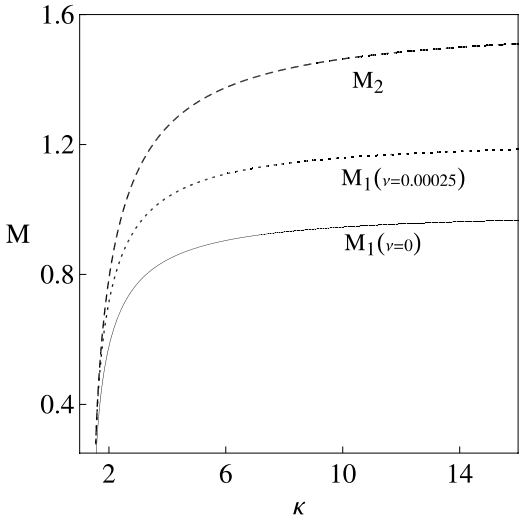

Figure 2. The 'allowed' solitary wave speed (Mach number M) range of values: the IA soliton existence domain (delimited by M_1 and M_2) is depicted in the κ–M parameter plane, for $U_0 = 0.05$. From top to bottom, the dashed curve (upper limit) corresponds to the infinite compression limit M_2, for $\nu = 0.000\,25$, *or* $\nu = 0$ (no noticeable dependence of M_2 on ν; see the discussion following equation (33) in the text); the dotted curve (lower limit) to threshold M_1 for $\nu = 0.000\,25$ and the solid curve to threshold M_1 for $\nu = 0$ (no beam). Recall that solitons may occur in the region between the top and middle curves for beam-plasma or between the top and bottom curves, for ordinary (e–i) plasmas.

known upper limit $M_2^{(\mathrm{e-i})} \simeq 1.58$ for IA solitons in e–i plasmas [2]. Keeping $\nu = 0$ (no beam) but $\kappa < \infty$ (superthermal electrons), equation (32) recovers exactly equation (22) in [44].

Now, let us consider ν to be finite (non-zero). Recalling that $U_0 \ll M < M_2$ and $\mu,\ \nu \ll 1 \leqslant Z$ are assumed to hold, we obtain from equation (32) the approximate relation:

$$\left(1 - \nu\sqrt{\frac{\mu}{Z}}\right) M_2^2 + \left[1 - \left(1 - \frac{M_2^2}{2\kappa - 3}\right)^{-\kappa+3/2}\right] = 0, \tag{33}$$

where a (small) contribution of the order $\sim \mathcal{O}[(U_0/M_2)^2]$ is omitted. Given the smallness of ν, μ and U_0, we conclude that M_2 (upper curve) in figure 2 does not change essentially by varying ν nor U_0.

4.3. Parametric investigation

We have seen that IA solitary waves, in the form of electric potential excitations (pulses), exist for values of the soliton speed (Mach number) M in the range $M_1 < M < M_2$. Since both of these limits vary with κ, ν and U_0, it is appropriate to investigate their dependence on these physical parameters. We have considered $Z = 1$ for this study.

The range of permitted values for the soliton speed (Mach number) M is elucidated in figure 2, which depicts the variation of the lower and upper limits M_1 and M_2 with κ (for representative fixed values of the density ratio ν and beam velocity U_0). Recall that solitons may be sustained in the region in between these two limits. The upper curve in figure 2 (for $\nu = 0$ and $\nu = 0.000\,25$) represents the upper velocity limit (M_2) for the existence of solitons, beyond which no soliton can be sustained. This corresponds to the infinite compression limit, where the density ceases to be real. Further variation of the value of ν, i.e. of the beam density, (within physically acceptable limits) produces no significant change to this curve. The middle

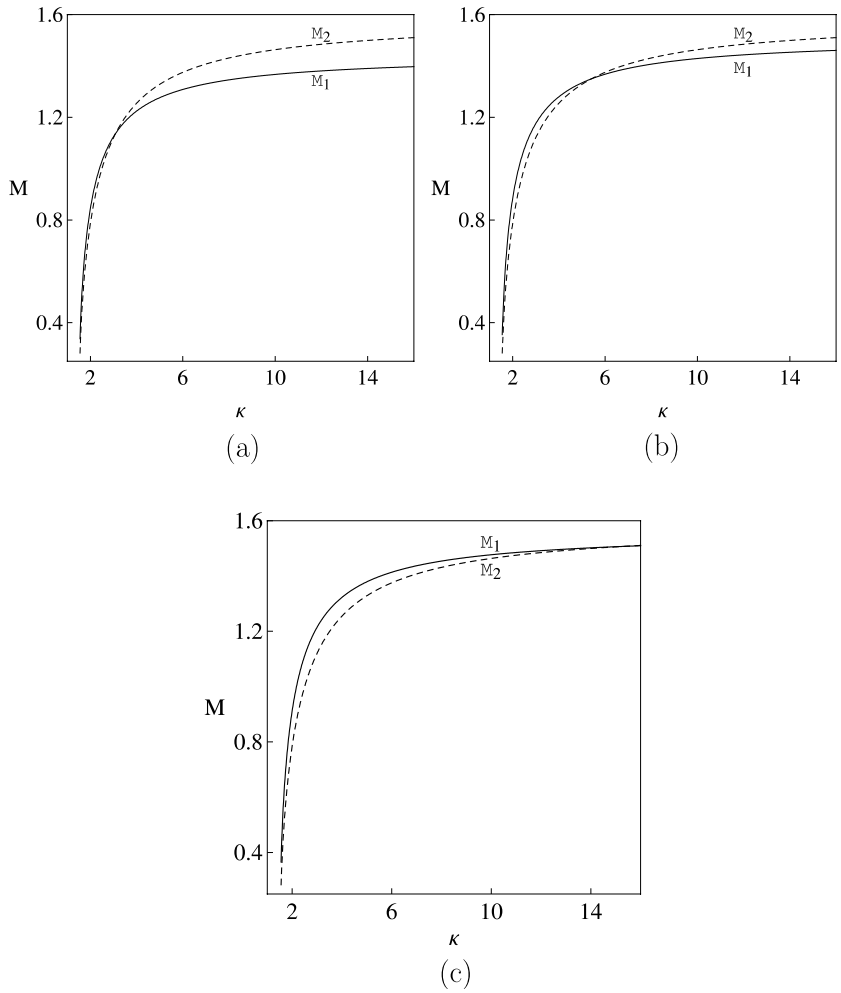

Figure 3. Variation of the Mach number M with κ for $U_0 = 0.05$ and with the electron-beam-to-ion density ratio (ν) (*a*) $\nu = 0.0005$, (*b*) $\nu = 0.000\,65$ and (*c*) $\nu = 0.000\,73$. The solid curve corresponds to M_1 and the dotted curve to M_2.

curve in figure 2, for $\nu = 0.000\,25$, corresponds to the (real, κ-dependent) sound speed threshold M_1. The lower curve in the same plot depicts the same sonic threshold for $\nu = 0$, i.e. with no beam. Both Mach number M limits (i.e. M_1 and M_2) increase with an increase in the values of κ and beam parameter ν. Numerically, we find that M_2 approaches 1.58 (upper velocity limit) and $M_1 = 1$ (lower velocity limit), in the limit $\kappa \to \infty$ and $\nu \to 0$ (see figure 2), thus recovering the long-known values predicted in the seminal work by Sagdeev in [2].

No ES solitary waves occurrence for small κ and high ν values. Here is a most interesting point to be made. Having noticed (in figure 2) that the lower M boundary (M_1) increases with higher beam density ν, one is tempted to investigate whether—for reasonably high values of ν—the sonic threshold M_1 might reach—or exceed—the upper limit M_2. Indeed, the answer is affirmative, as we show in figures 3(*a*)–(*c*). For instance, for $\nu = 5 \times 10^{-4}$, the 'lower' curve M_1 in fact lies *above* the 'upper' one M_2, suggesting that there are *no* solitary waves for κ below, say, $\simeq$3.5 (see figure 3(*a*)). The κ threshold is twice as high for $\nu = 6.5 \times 10^{-4}$ (see figure 3(*b*))

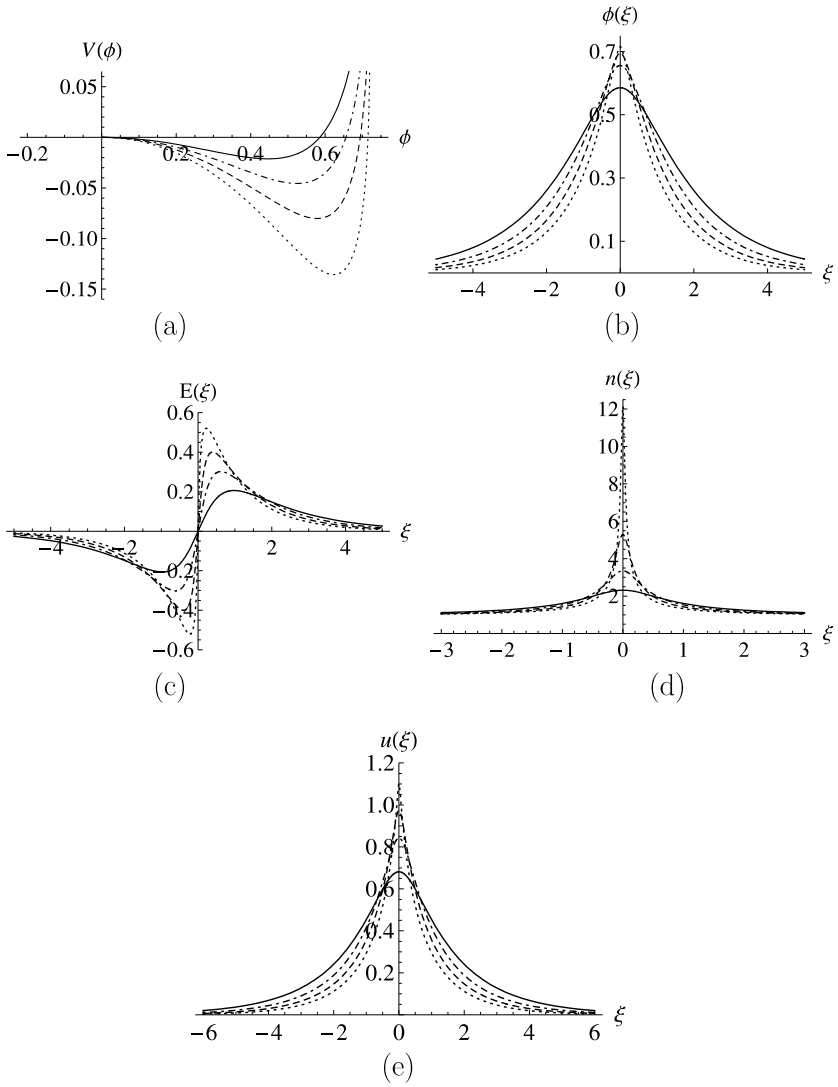

Figure 4. For $\nu = 0.000\,25$, $U_0 = 0.05$, $M = 1.2$ and different values of κ. Variation of (a) $V(\phi)$ versus ϕ, (b) the IA potential ϕ versus ξ, (c) the electric field E versus ξ, (d) the number density of ion n versus ξ and (e) the ion fluid velocity u versus ξ. The dotted curve corresponds to $\kappa = 4$; dashed curve to $\kappa = 5$; dotted–dashed curve to $\kappa = 7$; solid curve to $\kappa = 16$.

and increases high enough to include the quasi-Maxwellian region beyond $\nu = 7.3 \times 10^{-4}$ (see figure 3(c)). We therefore deduce that although ES solitary waves may occur in Maxwellian plasmas penetrated by an electron beam, they are plainly invalidated by superthermality (low κ). This effect is clearly related to the electron beam, i.e. is not present for $\nu = 0$.

5. Solitary waves: form and characteristics

We have numerically solved the energy-balance equation (28) (combined with equation (29)), for various values of κ, Mach number and beam velocity U_0, with fixed values of other plasma parameters. These results are shown in figures 4–10.

Superthermality effect (via κ). We recall that the deviation from the Maxwellian profile of the electron background is measured via the value of the spectral index κ. To show the effect of superthermality, we have considered different values of κ, from small (near the minimum of 3/2) up to large ones (recall that values above $\sim$10 are practically tantamount to a Maxwellian). The corresponding pseudopotential $V(\phi)$ is depicted in figure 4(a), while the associated pulse (potential ϕ) solitons, ambipolar electric field (E) structure, ion fluid density (n) and fluid speed (u) (obtained numerically) are depicted in figures 4(b)–(e), respectively. In figure 4(a), we see that the root of $V(\phi)$ (maximum ES potential) ϕ_0 increases monotonically with an increase in superthermality (i.e. a decrease in the values of κ) as seen upon a simple comparison of the curves (top to bottom). The depth of the Sagdeev potential well increases with an increase in superthermality (decrease in κ). We recall that the depth of the pseudopotential corresponds to the maximum value of $\phi'(\xi)$ (via equation (28)), so a deeper well implies a steeper (narrower) soliton pulse. Therefore, superthermality is expected to lead to narrower pulses (less extended spatially) being observed. The Mach number threshold M_1 increases with higher values of the beam-to-ion density ratio ν and/or the beam velocity U_0. The values chosen for this plot are associated with pulse profiles of the ES potential ϕ, which are depicted in figure 4(b) (for the same values of κ, ν and U_0, as in figure 4(a)). The amplitude (width) of the IA soliton is seen to increase (decrease, respectively) with stronger superthermality (i.e. a decrease in the value of κ)—see figure 4(b), entailing a similar variation of the electric field E (see figure 4(c)), ion density n (figure 4(d)) and velocity u (figure 4(e)).

Negative potential pulses. It is known from previous studies that the coexistence of inertial species of opposite charge polarity in a plasma may result in the (co-)existence of excitations of opposite polarity as well, i.e. of potential disturbances of either plus or minus sign (e.g. the coexistence of positive and negative potential IA solitary waves may occur either with the presence of two electron (Maxwellian) populations [58–60] or with single nonthermal electron in plasma) [61, 62]. We have so far anticipated positive IA pulses. One is therefore tempted to search for negative polarity potential structures as well, as intuitively suggested here by the coexistence of an electron fluid (the beam) with the inertial ions. Indeed, negative solitary waves do exist, in fact in the same—or at least partly overlapping—parameter regions (i.e. under the same physical conditions, or part thereof) as the positive IA pulses studied above. This is obvious in figure 5(a), where we have adopted the same set of parameters as in figure 4(a). The maximum amplitude of these negative structures is very small, compared with the positive potential structures. Here also, the maximum amplitude of (negative) solitary waves increases with an increase in superthermality (i.e. a decrease in the value of κ). The pulse profile for ES potential ϕ is depicted in figure 5(b). The dependence of the pulse amplitude and width on the value of κ is similar to that of the positive potential solitary waves case (e.g. see figure 4(b)).

Soliton speed (M) effect. Figure 6(a) shows the variation of the Sagdeev potential $V(\phi)$ versus ϕ for different values of the soliton speed (Mach number M) with $\kappa = 4$, and keeping other plasma parameters fixed. The maximum ES potential ϕ_0 increases with an increase in M. In figure 6(b), we have depicted the variation of the potential ϕ pulse profile for different values of M, keeping the remaining plasma parameters as in figure 6(a). It is seen that the soliton speed is related to the solitary structures' characteristics, so that in fact faster solitons are taller and steeper, in agreement with the usual picture.

Beam density (ν) effect. It is interesting to point out that the (region of allowed values of the) soliton speed M moves to higher values with an increase in ν (see figure 1(a)). Since the

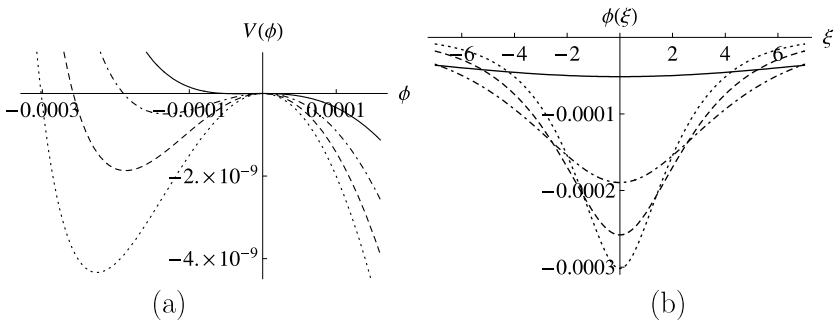

Figure 5. For negative potential solitary waves: variation of (*a*) $V(\phi)$ versus ϕ, and (*b*) the IA potential ϕ versus ξ for the other same parameters as in figure 4. The dotted curve corresponds to $\kappa = 4$; dashed curve to $\kappa = 5$; dotted–dashed curve to $\kappa = 7$; solid curve to $\kappa = 16$.

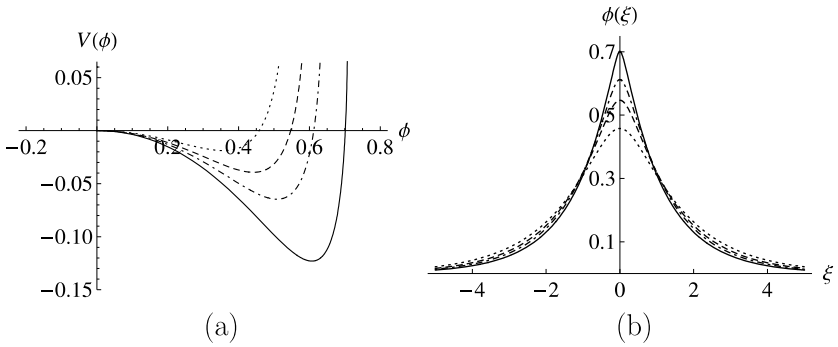

Figure 6. Variation of (*a*) $V(\phi)$ versus ϕ and (*b*) the IA potential ϕ versus ξ, for different values of the Mach number (M) and $\nu = 0.000\,25$, $U_0 = 0.05$, $\kappa = 4$. Dotted curve: $M = 1.04$; dashed curve: $M = 1.09$; dotted–dashed curve: $M = 1.13$ and solid curve: $M = 1.19$.

amplitude depends on the propagation speed, one therefore expects to find a dependence of the amplitude on the beam characteristics (density, velocity). Indeed, an increase in ν (implying, as said earlier, an increase in the prescribed soliton speed) thus leads to an increase in the maximum amplitude ϕ_0. The maximum amplitude of *negative* solitary waves turns out to be a growing function of the beam density ν. Therefore, for negative ϕ_0, the absolute value of ϕ_0 (the amplitude of the negative pulses see figure 7(*a*)) decreases with increasing ν. As one might expect, therefore, the negative amplitude vanishes above a certain value of ν (an upper limit). For instance, we have found numerically that the negative potential solitary waves disappear for a value of $\nu \geqslant 5 \times 10^{-4}$, assuming $\kappa = 4$, $M_1 = 1.2$ and $U_0 = 0.05$. On the other hand, *positive* potential solitary waves undergo a negligible change, if any, in their amplitude (a decrease, in fact), by varying the beam density; see figure 7(*b*), where a variation of less than 0.1% is observed, for a beam twice as dense or higher.

Beam velocity (U_0) effect. In the absence of the beam, an unmagnetized plasma is isotropic. Therefore, no loss of generality is implied by considering any sign of (the soliton speed) M. However, 'switching on' an electron beam leads to symmetry-breaking, in the sense that there is a particular direction (that of the beam flow) which distinguishes between a positive and a negative direction along the x-axis (in a 1D geometry). A distinction among solitary wave excitations which are co- and counter-propagating (with respect to the beam) needs to be made

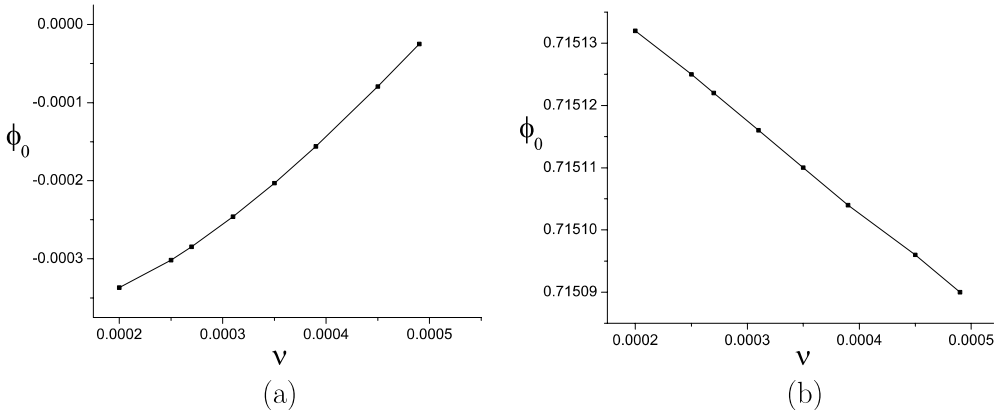

Figure 7. Variation of the maximum ES potential ϕ_0 versus ν for $\kappa = 4$, $M = 1.2$ and $U_0 = 0.05$. (*a*) For negative potential structures and (*b*) for positive potential structures.

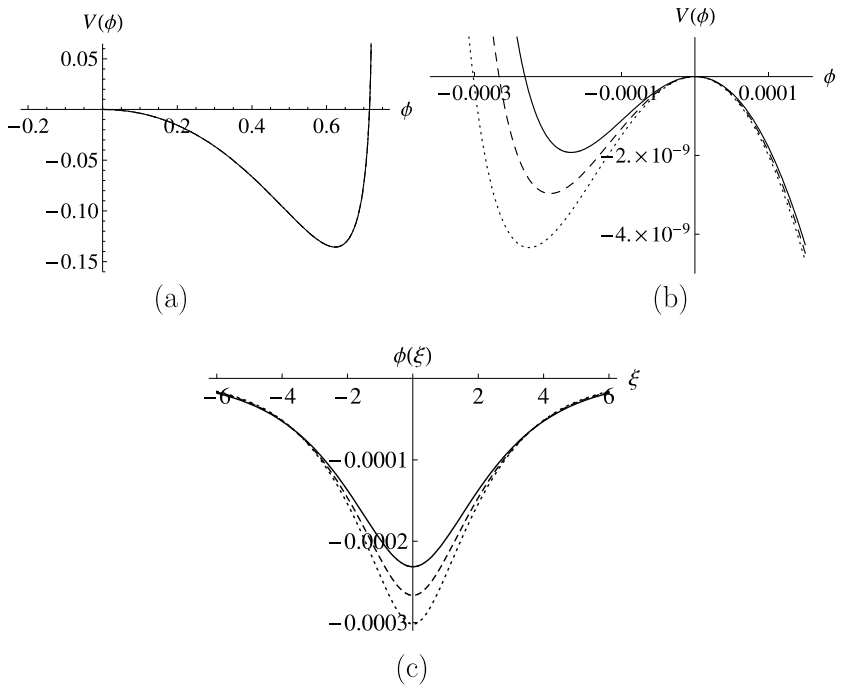

Figure 8. For solitary wave propagating in the direction of electron beam flow: variation of (*a*) (and (*b*)) $V(\phi)$ versus ϕ and (*c*) the IA potential ϕ versus ξ, for different values of the beam velocity (U_0) and $\nu = 0.000\,25$, $\kappa = 4$ and $M = 1.2$. The dotted curve: $U_0 = 0.05$; dashed curve: $U_0 = 0.09$; solid curve: $U_0 = 0.13$.

in the analysis. These cases can be studied by considering negative values of either U_0 or M. We have chosen to do the former, by assuming a given Galilean frame $\xi = x - Mt$ and thus considering separately positive and negative values of U_0.

Let us first consider solitary waves propagating in the direction of the electron beam flow. Figures 8(*a*) and (*b*) depict the variation of the Sagdeev potential $V(\phi)$ versus ϕ for different values of the beam velocity U_0. Since the charge current entering Ampére's law is essentially $J = \nu U_0$ (in reduced form), the beam velocity U_0 effect is essentially similar to that of the beam

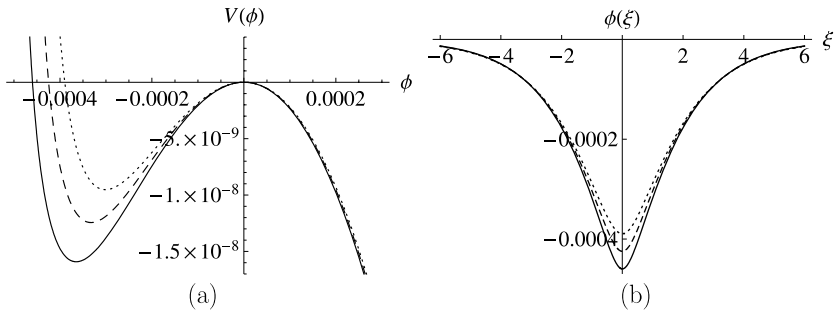

Figure 9. For counter-propagating solitary wave: variation of (*a*) $V(\phi)$ versus ϕ and (*b*) the IA potential ϕ versus ξ, for different values of the beam velocity (U_0) and $\nu = 0.000\,25$, $\kappa = 4$ and $M = 1.2$. Dotted curve: $U_0 = -0.05$; dashed curve: $U_0 = -0.09$; solid curve: $U_0 = -0.13$.

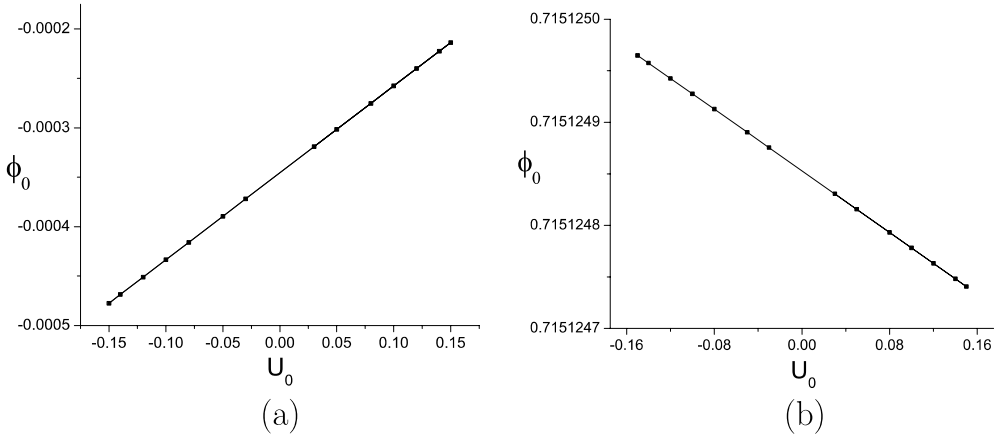

Figure 10. Variation of the maximum ES potential ϕ_0 versus U_0 for $\kappa = 4$, $M = 1.2$ and $\nu = 0.000\,25$. (*a*) For negative potential structures and (*b*) for positive potential structures.

density ν (discussed above). Negative potential solitary waves decrease in amplitude with an increase in the beam velocity U_0, while there is no noticeable change for positive potential structures. Note for instance that the three curves (for different U_0 values), for positive pulses, coincide exactly in figure 8(*a*) (i.e. overlapping, cannot be distinguishable); compare this to figure 8(*b*) for negative pulses. This suggests a negligible dependence of positive solitons on the beam velocity U_0. In figure 8(*c*), we have depicted the variation of the potential ϕ pulse profile for different values of U_0 (fixing the remaining plasma parameters as in figure 8(*a*)). It is seen that a higher beam velocity leads to a decrease in the solitary wave amplitude and to an increase in its width. The behaviour described in this paragraph is also observed in figure 10 (considering positive U_0 values therein).

In order to take into account *counter-propagating* solitary waves (i.e. propagating in the direction opposite to the electron beam), we have also considered negative values of the beam velocity U_0. Figure 9(*a*) shows the variation of the Sagdeev potential $V(\phi)$ versus ϕ for different negative values of the beam velocity U_0. Again, negative potential solitary waves increase in amplitude for higher beam velocity U_0, yet there is no noticeable change in the potential variation of positive potential structures. The variation of the potential ϕ pulse profile for different negative values of U_0 is shown in figure 9(*b*), by keeping the remaining plasma parameters as in figure 9(*a*). The increase in the negative value of beam velocity leads to an

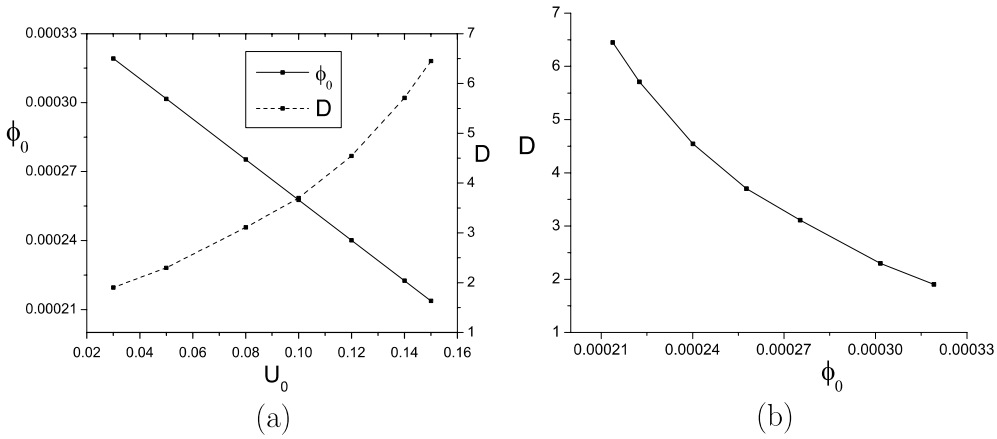

Figure 11. For $\kappa = 4$, $M = 1.2$ and $\nu = 0.000\,25$, variation of (a) the soliton amplitude ϕ_0 and width parameter D versus the beam velocity U_0 and (b) the soliton width parameter D versus the soliton amplitude ϕ_0 obtained for different values of the beam velocity U_0.

increase in amplitude (and a decrease in width). Therefore, the *inverse* effect is now witnessed, as compared with the behaviour obtained above for *co-propagating* solitary waves.

The behaviour discussed in the latter two paragraphs is in fact summarized in figure 10. In figure 10(a), we have depicted the variation of the maximum ES potential ϕ_0 of negative potential solitary waves versus the beam velocity U_0 for solitary waves propagating either in the direction of the beam flow or opposite to it. The analogous plot for positive pulses is given in figure 10(b). We see that co-propagating negative ES potential pulses decrease in amplitude with an increase in the value of the beam velocity. In fact, when the beam velocity (U_0) approaches 0.4 (for $\kappa = 4$, $M_1 = 1.2$ and $\nu = 0.000\,25$, here), the negative potential solitary waves disappear. On the other hand, such (negative) pulses increase in amplitude for higher beam velocity in the counter-propagating case. Finally, from figure 10(b), we see that there is an infinitesimally small change (a slight decrease, in fact) in the amplitude ϕ_0 of positive potential solitary waves (pulses) with an increase in the beam velocity (regardless of its direction); in fact, a change by a factor of the order of 10^{-6} or less (0.0001%) is obtained in the amplitude, for the values considered.

The root of $V'(\phi)$, say ϕ_1, relates to $\mid V(\phi_1) \mid^{-1}$ (the depth of the potential well) and to the soliton's curvature points ($\phi''(\xi) = 0$), so we evaluate $1/ \mid V(\phi_1) \mid$ versus $\mid \phi_0 \mid$. The deeper the $V(\phi_1)$, the steeper/narrower the soliton (ϕ_0) is. The soliton width parameter is $(D) = 1/ \mid V(\phi_1) \mid$ and its variation is shown in figure 11. Figure 11(a) depicts the variation of the width parameter D and the soliton amplitude ϕ_0 with the beam velocity U_0. It is seen that the width parameter (soliton amplitude) increases (decreases) with an increase in the beam velocity U_0. Hence the width parameter which represents the variation of the soliton width decreases with an increase in the amplitude of the soliton (figure 11(b)). It may be added for rigour that the depth of the pseudopotential well was here associated with the width heuristically, as explained above. The same may well be measured from the potential profiles (as in our plots) numerically, providing the same qualitative results.

6. Conclusions

We have provided a thorough analysis from first principles of the occurrence of large amplitude IA solitary waves in an unmagnetized plasma consisting of ions and excess superthermal

electrons (modelled by a kappa-type distribution), which is penetrated by an electron beam. A kappa (κ-) type distribution was assumed for the background electrons. A pseudopotential formalism was employed to derive an energy-balance like equation. The range of allowed values of the soliton speed (Mach number), wherein solitary waves may exist, was determined. We have traced the effect of superthermality and beam parameters (the beam-to-ion density ratio and the beam velocity) on the characteristics of IA solitary structures.

Our results are summarized as follows:

(i) Both large positive structures and small negative potential structures may (co-)exist.

(ii) The Mach number range for the existence of IA solitary waves sensitively depends on the ν, U_0 and superthermality (via κ). In the combined presence of the electron beam and superthermal (off-Maxwellian) electrons in the background, both lower and upper limit(s) of the soliton speed (M_1 and M_2) are modified. The plasma in general supports slower solitons for smaller values of κ (increased electron superthermality), yet faster ones for an increased beam current $j = \nu\, U_0$. The electron beam (density and velocity) parameters affect the lower threshold (M_1 increases for higher $j = \nu U_0$), yet have no significant effect on the upper limit (i.e. no change in the value of M_2). In the absence of the beam, the well-known previous limit (Mach number range in [44]) is retrieved. Furthermore, in the limit $\kappa \to \infty$ and $\nu \to 0$ (no beam), the predicted lower and upper limits agree with the results for e–i plasma with a Maxwellian electron distribution ($M \in [1, 1.58]$) [2].

(iii) For fixed Mach number and beam parameters, both soliton amplitude and the steepness of the soliton profile increase monotonically with a decrease in κ (i.e. increase in superthermality).

(iv) The electron beam effect essentially shrinks the region of permitted speed (Mach number M) values, but increases the values of both boundaries M_1 and M_2 (thus allowing for faster ES solitary waves). (The effect of the beam velocity on M is small as compared with that of the beam density.) M_1 increases with an increase in either beam density (ν) or velocity (U_0).

(v) *Interestingly,* under the combined effect of the electron beam and of the superthermal electrons, the Mach number range *may even be reduced to nil* for high enough beam density and low enough κ (significant superthermality).

(vi) In general, both soliton amplitude and (electric potential perturbation) profile steepness increase as κ decreases (for fixed values of all other parameters, i.e. Mach number, electron beam-to-ion density ratio and electron beam velocity). For fixed κ, an increase in soliton speed (M_1) leads to an increase in both amplitude and steepness profile of the solitary wave excitation(s).

This study may shed some light on the properties of IA solitary waves in space and laboratory plasmas (laser–matter/plasma interaction experiments), where the combined presence of electron beams and excess superthermal electrons may be encountered.

Acknowledgments

The authors are grateful to Professor F Verheest (Universiteit Gent, Belgium) and Professor M A Hellberg (University of Qwa-Zulu Natal, Durban, South Africa) for useful discussions. This work was supported by a UK EPSRC Science and Innovation award to Centre for Plasma Physics (CPP grant EP/D06337X/1). NSS gratefully acknowledges the leave granted by the authority of Guru Nanak Dev University, Amritsar, India.

References

[1] Washimi H and Taniuti 1966 *Phys. Rev. Lett.* **17** 996
[2] Sagdeev R Z 1966 *Rev. Plasma Phys.* **4** 23
[3] Ikezi H, Tailor R J and Basker D R 1970 *Phys. Rev. Lett.* **25** 11
Longren K E 1983 *Plasma Phys.* **25** 943
Nakamura Y, Ito T and Koga K 1993 *J. Plasma Phys.* **49** 331
[4] Witt E and Lotko W 1983 *Phys. Fluids* **26** 2176; see references [1–7] therein
[5] Temerin M 1982 *Phys. Rev. Lett.* **48** 1175
[6] Boström R 1988 *Phys. Rev. Lett.* **61** 82
[7] Ergun R E *et al* 1998 *Geophys. Res. Lett.* **25** 2061
Delory G T *et al* 1998 *Geophys. Res. Lett.* **25** 2069
Pottelette R *et al* 1999 *Geophys. Res. Lett.* **26** 2629
[8] McFadden J P *et al* 2003 *J. Geophys. Res.* **108** 8018
[9] Matsumoto H *et al* 1994 *Geophys. Res. Lett.* **21** 2915
Franz J R *et al* 1998 *Geophys. Res. Lett.* **25** 1277
Cattell C A *et al* 1999 *Geophys. Res. Lett.* **26** 2629
[10] Omura Y, Kojima H, Umeda T and Matsumoto H 2001 *Astrophys. Space Sci.* **277** 45
[11] Omura Y, Kojima H and Matsumoto H 1994 *Geophys. Res. Lett.* **21** 2923
[12] Yamagiwa K, Itoh T and Nakayama T 1997 *J. Physique IV France* **7** C4-413
[13] Takeda T and Yamagiwa K 2003 *J. Plasma Fusion Res.* **79** 323
[14] Takeda T and Yamagiwa K 2004 *J. Plasma Fusion Res. SERIES* **6** 566
[15] Giulietti D, Galimberti M, Giulietti A, Gizzi L A, Borghesi M, Balcou Ph, Rousse A and Rousseau J Ph 2001 *Phys. Rev.* E **64** 015402
[16] Moslem W M 1999 *J. Plasma Phys.* **61** 177
[17] Esfandyari A R, Khorram S and Rostami A 2001 *Phys. Plasmas* **8** 4753
[18] Esfandyari-Kalejahi A, Kourakis I, Dasmalchi B and Sayarizadeh M 2006 *Phys. Plasmas* **13** 042305
[19] Chatterjee P and Roychoudhury R 1995 *Z. Naturf.* **51a** 1002
[20] Nejoh Y and Sanuki H 1995 *Phys. Plasmas* **2** 4122
[21] Nejoh Y 1997 *J. Plasma Phys.* **57** 841
[22] Lu Q, Wang S and Dou X 2005 *Phys. Plasmas* **12** 072903
[23] Berthomier M, Pottelette R, Malingre M and Khotyaintsev Y 2000 *Phys. Plasmas* **7** 2987
[24] Sahu B and Roychoudhury R 2004 *Phys. Plasmas* **11** 1947
[25] El-Taibany W F and Moslem W M 2005 *Phys. Plasmas* **12** 032307
[26] Lakhina G S, Singh S V, Kakad A P, Verheest F and Bharuthram R 2008 *Nonlinear Process. Geophys.* **15** 903
[27] Esfandyari-Kalejahi A, Kourakis I and Shukla P K 2008 *Phys. Plasmas* **15** 022303
[28] Summers D and Thorne R M 1991 *Phys. Fluids* B **3** 1835
[29] Mace R L and Hellberg M A 1995 *Phys. Plasmas* **2** 2098
[30] Hellberg M A and Mace R L 2002 *Phys. Plasmas* **9** 1495
[31] Ryu C-M *et al* 2007 *Phys. Plasmas* **14** 100701
[32] Gaelzer R *et al* 2008 *AstroPhys. J.* **677** 676
[33] Schippers P *et al* 2008 *J. Geophys. Res.* **113** A07208
[34] Goldman M V, Newman D L and Mangeney A 2007 *Phys. Rev. Lett. J.* **99** 145002
[35] Hellberg M A, Mace R L, Armstrong R J and Karlstad G 2000 *J. Plasma Phys.* **64** 433
[36] Yoon P H, Rhee T and Ryu C-M 2005 *Phys. Rev. Lett.* **95** 215003
[37] Magni S *et al* 2005 *Phys. Rev.* E **72** 026403
[38] Nakatsutsumi M *et al* 2008 *New J. Phys.* **10** 043046
[39] Nakamura H *et al* 2009 *Phys. Rev. Lett.* **102** 045009
[40] Vasyliunas V M 1968 *J. Geophys. Res.* **73** 2839
[41] Leubner M P 2004 *Phys. Plasmas* **11** 1308
[42] Baluku T K and Hellberg M A 2008 *Phys. Plasmas* **15** 123705
[43] Menietti J D *et al* 2008 *J. Geophys. Res.* **113** A05213
[44] Saini N S, Kourakis I and Hellberg M A 2009 *Phys. Plasmas* **16** 062903
[45] Hellberg M A, Mace R L, Baluku T K, Kourakis I and Saini N S 2009 *Phys. Plasmas* **16** 094701
[46] Livadiotis G and McComas D J 2009 *J. Geophys. Res.* **114** A11308
Livadiotis G and McComas D J private communication
[47] Tsallis C 1988 *J. Stat. Phys.* **52** 479–87
[48] Boon J P and Tsallis C 2005 *Europhys. News* **36** 185

[49] Treumann R A 2001 *Astrophys. and Space Sci.* **277** 81
[50] Treumann R A, Jaroschek C H and Scholer M 2004 *Phys. Plasmas* **11** 1317
[51] Collier M R 2004 *Adv. Space Res.* **33** 2108
[52] Ergun R E *et al* 1998 *Geophys. Res. Lett.* **25** 2041
[53] Borghesi M *et al* 2002 *Phys. Rev. Lett.* **58** 135002
[54] Romagnani L *et al* 2008 *Phys. Rev. Lett.* **101** 025004
[55] See, e.g., the discussion in Verheest F 2009 *J. Phys. A: Math. Theor.* **42** 285501
[56] Verheest F, Hellberg M A and Lakhina G S 2007 *Astrophys. Space Sci. Trans.* **3** 15
[57] Bryant D A 1996 *J. Plasma Phys.* **56** 87
[58] Buti B 1980 *Phys. Lett.* A **76** 251
[59] Nishihara K and Tajiri M 1981 *J. Phys. Soc. Japan* **50** 4047
[60] Tagare S G 2000 *Phys. Plasmas* **7** 883
[61] Cairns R A *et al* 1995 *Geophys. Res. Lett.* **22** 2709
[62] Mamun A A 1997 *Phys. Rev.* E **55** 1852